Catalysis Letters Vol. 103, Nos. 1–2, September 2005 (© 2005)
DOI: 10.1007/s10562-005-6516-4

Activity patterns for the water gas shift reaction over supported precious metal catalysts

Yun Lei, Noel W. Cant, and David L. Trimm*

School of Chemical Engineering and Industrial Chemistry, The University of New South Wales, NSW, 2052 Australia

Received 26 March 2005; accepted 29 May 2005

Activity patterns for the high temperature water gas shift reaction over oxide catalysts promoted by precious metals show that the performance of iron oxide–chromia catalysts can be significantly improved by promotion with small amounts of rhodium. The results suggest that reactions of hydrogen at the promoter–catalyst interface are the rate controlling process.

KEY WORDS: water gas shift; precious metal promotion; Fe-Cr oxide catalysts for water gas shift.

1. Introduction

Despite the fact that the water gas shift (WGS) reaction was among the first catalytic processes to be developed on an industrial scale [1], questions still remain as to the kinetics and mechanism of the reaction over different catalysts. The thermodynamics of the reversible reaction are well established.

$$CO + H_2O \rightleftharpoons CO_2 + H_2 \qquad \Delta H = -41.09 \text{ kJ/mole} \tag{1}$$

with the production of hydrogen being favoured at low temperatures. Excellent reviews of various aspects of the reaction have been presented [2–6].

The most important industrial catalysts are based on iron oxide/chromium oxide, which are effective above ~350 °C, and copper/zinc oxide/alumina which deactivate above ~300 °C. There is some discussion as to the reaction mechanism over both catalysts. A redox mechanism [5,7]

$$MO_s + CO \rightarrow M\square_s + CO_2 \tag{2}$$

$$M\square_s + H_2O \rightarrow MO_s + H_2 \tag{3}$$

(where $\square_s$ is a surface vacancy) and a mechanism involving the formation and decomposition of an adsorbed formate [5,8]

$$CO_{ads} + H_2O_{ads} \rightarrow HCOOH_{ads} \tag{4}$$

$$HCOOH_{ads} \rightarrow H_2 + CO_2 \tag{5}$$

have been proposed.

The water gas shift reaction (WGS) has come into recent prominence in the context of fuel cells for automotive applications [5]. The most successful fuel cell (PEMFC) operates on hydrogen [9], originating from synthesis gas (H_2, CO) produced by reforming methane or some other fuel [3,9]. The concentration of carbon monoxide produced must be minimised to avoid poisoning the fuel cell electrode. WGS followed by selective oxidation are the preferred reactions to lower CO [9].

Precious metals catalysts are of particular interest in this application [7,10,11], with ceria supports – which promote oxygen storage and WGS – being of particular interest. Comparisons of WGS on ceria supported Pd, Pt and Rh [7] and Pd, Ni, Fe, Co and Pt [10] suggest that CO adsorbs on the metal and reacts with oxygen from the ceria which, in turn, is reoxidised by water [12].

The present paper reports a survey of higher temperature WGS over precious metals supported on a range of oxidic supports, including iron oxide/chromium oxide. Precious metal promotion of such systems has not been reported previously but there is one recent report concerning promotion of Fe_3O_4/Cr_2O_3 by base metals with Hg and Ba-containing catalysts showing the highest activities [13].

2. Experimental

Most of the support oxides (those based on Fe, Cr, Mn, Mg, Ce and Zr) were prepared by precipitation from aqueous nitrate salts (AR, Aldrich) by slow addition of solutions of NH_4OH (30%, AR, Aldrich) or Na_2CO_3 (AR, Aldrich). The resultant hydroxides or carbonates were washed, filtered, dried and calcined in air for 3 h at 500 °C. Bi_2MoO_6 was made by the slurry phase reaction between $Bi(NO_3)_3$ and molybdic acid under acidic conditions [14]. The MoO_3 and V_2O_5 were commercial samples (Ajax Chemicals), as was the γ-Al_2O_3 (Norton, type SA-6173), U_3O_8 was made by direct decomposition of solid uranyl nitrate in air for 5 h at 800 °C.

---

* To whom correspondence should be addressed.
E-mail: d.trimm@unsw.edu.au

Taking preparation of Fe_2O_3–Cr_2O_3 as an example, the catalyst preparation involved precipitating $Fe(OH)_3$ from iron nitrate by adding 30% ammonia hydroxide to a pH of 7.5–8.0. The precipitate was filtered and washed before preparing a thick slurry. Chromium nitrate solution was then stirred into the slurry (pH 7.5–8.0) and the mixture was aged for 8 h. After filtration and washing the solid was dried (110 °C, 16 h) and calcined (500 °C, 3 h). Samples crushed and sieved to various particle sizes were impregnated with rhodium nitrate using the incipient wetness technique, The final catalyst was dried and calcined as above.

Metals (1 wt% in each case) were deposited by wet impregnation using solutions of metal nitrates, with the exception of H_2PtCl_6, followed by a further calcination of the dried product for 3 h at 500 °C. Total surface areas were measured using a Micromeritics Tristar 2000 surface area analyser operated in the single point mode.

Activity testing was carried out using a flow system with catalyst samples of particle size not larger than 250 μm (weighing either 0.05 or 0.10 g) diluted 5:1 with 150 to 250 μm particles of inert α-Al_2O_3 and contained in a 10-mm internal diameter stainless steel tube. The feed stream comprised a standard CO/N_2 mixture (from BOC, Australia) to which water was added *via* a vapouriser fed by a high precision syringe pump (ISCO Inst., model 260D). The product stream, after passage through a trap at 0 °C to remove most of the water, was analysed using two gas chromatographs (Shimadzu GC8A) fitted with thermal conductivity detectors. One chromatograph was operated with helium passing through a 1.8 in CTR-1 column (Alltech Associates, Inc) for analysis of CO_2, CO, N_2, trace O_2 and CH_4, The other used argon passing through a 2 m molecule sieve 13X column for H_2 analysis.

The standard test stream comprised 9% CO, 9% H_2O balance N_2 with flow rates of 150 to 600 cm^3 (STP)/min discharging at atmospheric pressure. Each catalyst was pretreated in 10% H_2/N_2 (50 ml/min (STP)) with the temperature ramped to 400 °C at not greater than 5 °C per minute and held at 400 °C for 1 h. Catalysts were then stabilised in the standard feed at 350 °C for a minimum period of 1 h. Activities were determined by operation at several flow rates, first at higher temperatures (500 °C), then at lower temperatures, and finally at 350 °C again. The rate at each temperature was calculated from the initial slope of plots of CO conversion (X) versus the reciprocal of the flow rate in the differential region (at least one, and usually several, values of X below 20%).

3. Results and discussion

Experimental testing was carried out under condition that favoured the forward reaction between carbon monoxide and water. Typical Arrhenius plots for 1 wt% Pt supported on single component oxides are shown in figure 1. Most plots are parallel with some of the most active catalysts exhibiting curvature at high temperature, indicative of mass transfer restrictions [15].

Table 1 shows data for the full set of Pt-containing catalysts in descending order of activity. Activation energies cluster around 50 kJ/mol but with substantially lower values for Pt/ZrO_2 and Pt/CeO_2–ZrO_2. Rates at 450 °C vary by more than an order of magnitude with Pt/Al_2O_3 the least active and Pt/Cr_2O_3, Pt/Cr_2O_3–Fe_3O_4 and Pt/U_3O_8 the most active. Comparison with the data for the support oxides (the indented entries in the first column) shows that the extent of synergistic effects between Pt and the oxides varies widely. Cr_2O_3–Fe_3O_4 is by far the most active support and the increase in activity when Pt is present is limited to ~20%. Indeed the combined activity is little more than the sum of that attributable to the support alone and the Pt alone (as represented by Pt/Al_2O_3), On the other hand the activities of Pt in combination with Cr_2O_3, U_3O_8 and CeO_2–ZrO_2 are five, six and four times greater respectively than those expected from the sum of the activities of the oxide and Pt. In stark contrast to the substantial promotion evident for the Pt/Cr_2O_3 system, the activity of Pt/Fe_3O_4 is less than that expected for Fe_3O_4 and Pt taken together.

The effect of different metals as promoters was then examined using Cr_2O_3-Fe_3O_4 and Cr_2O_3 as supports (Figure 2). Rh/Cr_2O_3–Fe_3O_4 is the most active catalyst with clear evidence of mass transfer control suggested by the fact that the activation energy halved in going from the two lowest temperatures to the two highest (Table 2). The rate at 350 °C is almost twice that of the next most active (Pt/Cr_2O_3). It is also apparent that Pd, Ni and Cu, like Pt, promote Cr_2O_3–Fe_3O_4 only marginally. Likewise Ni does not promote Cr_2O_3 but Rh is almost as effective as Pt.

WGS over precious metal promoted ceria catalysts is generally believed to proceed *via* the redox mechanism, reactions (2) and (3) above [7,10,11]. The rate controlling process is suggested to involve transfer of oxygen across the surface of the support to react with CO adsorbed on the metal.

The present results suggest that transfer of oxygen across the support surface is not always rate controlling. Apparent activation energies are found to be remarkably similar (ca. 50 kJ/mole) for Pt supported on CeO_2, Cr_2O_3–Fe_3O_4, CeO_2–Fe_3O_4, Fe_3O_4, V_2O_5, MgO, MnO_x and Al_2O_3, despite up to 15-fold differences in rates of reaction (Table 1). It seems unlikely that surface diffusion of oxygen, if it was rate controlling, should show similar apparent activation energies for such a wide range of supports.

As a result, rates of reaction and apparent activation energies were measured using different promoters suspended on Cr_2O_3–Fe_3O_4 and on Cr_2O_3 and compared with literature values for CeO_2 [7,10] (Table 2). It is

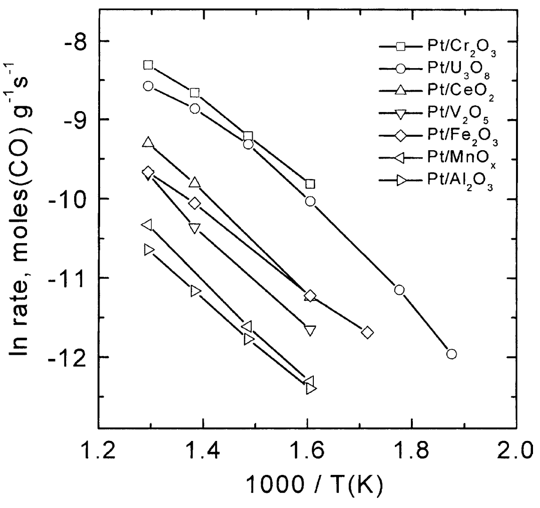

Figure 1. Arrhenius plots for the water gas shift reaction over single component oxide promoted with 1 wt% Pt.

Table 1
Rates and, apparent activation energies for water gas shift over 1% Pt/oxide catalysts

Catalyst	BET area ($m^2\ g^{-1}$)	Rate at 450 °C (mmol(CO) $g_{catalyst}^{-1}s^{-1}$)	E_a (kJ/mol)
Pt/Cr_2O_3	22	0.174	41 ± 2
Cr_2O_3		0.022	78 ± 1
$Pt/Cr_2O_3–Fe_3O_4$[a]	63	0.149	50 ± 3
$Cr_2O_3–Fe_3O_4$[a]		0.124	70 ± 2
Pt/U_3O_8	2.3	0.142	59 ± 3
U_3O_8		0.010	24 ± 2
$Pt/CeO_2–ZrO_2$[a]	67	0.079	28 ± 1
$CeO_2–ZrO_2$[a]		0.008	55 ± 1
$Pt/CeO_2–Fe_3O_4$[a]	n.m.[b]	0.070	50 ± 1
Pt/CeO_2	122	0.055	52 ± 1
Pt/MgO	77	0.034	41 ± 1
Pt/V_2O_5	6	0.032	52 ± 3
Pt/ZrO_2	n.m.[b]	0.026	24 ± 1
Pt/Fe_3O_4	29	0.022	55 ± 3
Fe_3O_4		0.023	48 ± 2
Pt/MoO_3	1.6	0.020	49 ± 3
Pt/Bi_2MoO_6	2.1	0.018[c]	62 ± 4
Pt/MnO_2	17	0.016[c]	53 ± 2
Pt/Al_2O_3	272	0.014	47 ± 1

[a] The composition of the mixed oxides were as follows: 8 wt% $Cr_2O_3–Fe_3O_4$, 8 wt% $CeO_2–Fe_3O_4$, 50 wt% $CeO_2–ZrO_2$.

[b] Not measured.

[c] No measurement at 450 °C, calculated from Arrhenius parameters.

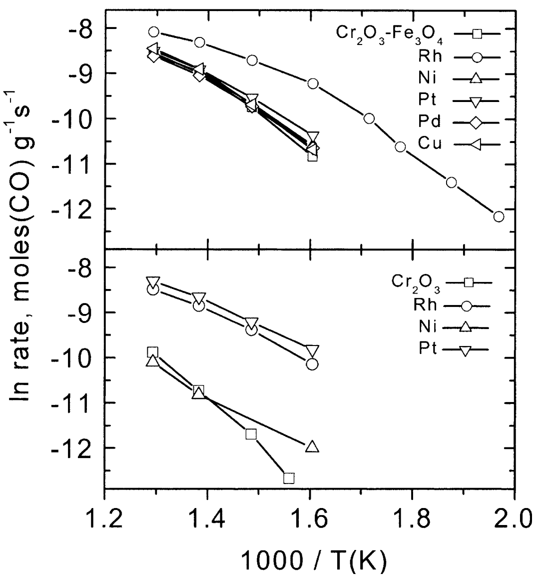

Figure 2. Arrhenius plots for the water gas shift reaction over metal-promoted Cr_2O_3-Fe_3O_4 and Cr_2O_3 catalysts.

Table 2
Activation energies for 1 wt% metal-promoted water gas shift catalysts

metal	$Cr_2O_3–Fe_3O_4$ E_a (kJ/mole)	Cr_2O_3 E_a (kJ/mole)	CeO_2 E_a (kJ/mole)
none	70 ± 2	78 ± 1	63[a]
Pt	50 ± 3	41 ± 2	46[a]
Pd	55 ± 4	–	46[a]
Rh	31(≥400 °C) 68 (≤300 °C)	44 ± 3	46[a]
Ni	54 ± 4	49 ± 5	44[b]
Cu	60 ± 4	–	–

[a] Data from reference [7].

[b] Data from reference [10].

clear that promoted Cr_2O_3 and CeO_2 are associated with similar values of apparent activation energy but that promoted Cr2O3–Fe_3O_4 gives higher values of apparent activation energy which differ between promoters (Table 2). At least in this case, it would seem that the promoter has a significant role.

The importance of the redox mechanism in these high temperature catalysts has been confirmed by Boreskov [17] who showed that the Fe^{2+}/Fe^{3+} couple existed in Cr_2O_3-Fe_3O_4 catalysts, with Fe^{2+} being oxidised to Fe^{3+} by water and Fe^{3+} being reduced by carbon monoxide.

It could then be argued that the role of the promoter was to accelerate the dissociation of water and, as a result, the oxidation of Fe^{2+}. Some support for this concept is derived from the knowledge that urania, a support that shows high activity when promoted (Table 1), favours water dissociation [3]. Precious metals also accelerate the hydrogen–water exchange reaction [18] and this would be expected to show the same trend as water dissociation. However, the relative efficiency of H_2/H_2O exchange (Pt > Rh > Pd) is not in agreement with the promotional trend for WGS (Rh > Pt > Pd).

Similarly, precious metals could be expected to increase adsorption of CO and possibly to favour migration of adsorbed gas to the metal–support interface [10]. The strength of adsorption of CO on metals (Pd > Rh > Fe > Pt > Ni > Cu) [19] is such that the WGS promotional activity (Rh > Pt > Pd∼Ni > Cu) has no obvious correlation.

Finally, it could be suggested that the role of the precious metal is to accelerate the combination and desorption of hydrogen atoms. This has been suggested not to be rate limiting above room temperature [20], the rate being controlled more by spillover from Rh or surface diffusion of the hydrogen atoms. In that it is clear that both the support/catalyst and the promoter can affect the efficiency of the WGS, the obvious inference is that the reaction rate is controlled at the promoter–support interface. A full study of the kinetics and mechanisms of the high temperature reaction over carefully characterised catalysts is in progress in order to explore this suggestion.

4. Conclusions

Activity patterns have been measured for precious metals supported on various oxides and used to promote the high temperature water gas shift reaction. Platinum is found to increase the reactivity of the catalysts, with promotional effect being most obvious with Cr_2O_3, U_3O_8 and CeO_2-ZrO_2 supports. Rh is found to be most active promoter for Fe–Cr oxides and for Cr_2O_3. The evidence suggests that the enhancement of rate involves reaction at the promoter–support interface.

Acknowledgments

This work was supported by a grant provided by the Australian Research Council.

References

[1] BASF, German Offen 254,572 (1911).
[2] D.S. Newsome, Catal. Rev. - Sci. Eng. 21 (1980) 275.
[3] M.V. Twigg, *Catalyst Handbook* (Wolfe Scientific, London, 1989).
[4] D.C. Grenoble, M.M. Estadt and D.F. Ollis, J. Catal. 67 (1981) 90.
[5] C. Rhodes, G.J. Hutchings and A.M. Ward, Catal. Today 23 (1995) 43.
[6] R.L. Keiski, T. Salmi, P. Niemesto, J. Ainassaari and V.J. Pohjola, Appl. Catal. A: General 137 (1996) 349.
[7] T. Bunluesin, R.J. Gorte and G.W. Graham, Appl. Catal. B 15 (1998) 107.
[8] T. Shido and Y. Iwasawa, J. Catal. 141 (1993) 71.
[9] D.L. Trimm and Z.I. Onsan, Catal. Rev. - Sci. Eng. 43 (2001) 31.
[10] S. Hilaire, X. Wang, T. Luo, R.J. Gorte and J. Wagner, Appl. Catal. A: General 215 (2001) 271.
[11] T. Giroux, S. Hwang, Y. Liu, W. Ruettinger and L. Shore, Appl. Catal. B 55 (2005) 185.
[12] C. Padeste, N.W. Cant and D.L. Trimm, Catal. Lett. 18 (1993) 305.
[13] C. Rhodes, B.P. Williams, F. King and G.J. Hutchings, Catal. Commun. 3 (2002) 381.
[14] Batist P.A., J.H.F. Bouwens and G.C.A. Schuit, J. Catal. 25 (1972) 1.
[15] J.M. Thomas and W.J. Thomas, *Principles and Practice of Heterogeneous Catalysis* (VCH, Weinheim, 1997).
[16] T. Bunluesin, H. Cordatos and R.J. Gorte, J. Catal. 157 (1995) 222.
[17] G.K. Boreskov, Kinet. Catal. 11 (1970) 374.
[18] N.H. Sagert and R.M.L. Pouteau, Can. J. Chem. 52 (1974) 2960.
[19] Bradford M.C.J. and M.A. Vannice, Ind. Eng. Chem. Res. 35 (1996) 3171.
[20] D. Martin and D. Duprez, J. Phys. Chem. 101 (1997) 4428.